# A combined spectroscopic and theoretical study of propofol·$(H_2O)_3$

Iker León, Emilio J. Cocinero, Judith Millán, Anouk M. Rijs, Imanol Usabiaga, Alberto Lesarri, Fernando Castaño, and José A. Fernández'

Citation: The Journal of Chemical Physics **137**, 074303 (2012); doi: 10.1063/1.4743960
View online: http://dx.doi.org/10.1063/1.4743960
View Table of Contents: http://aip.scitation.org/toc/jcp/137/7
Published by the American Institute of Physics

# A combined spectroscopic and theoretical study of propofol · $(H_2O)_3$

Iker León,[1] Emilio J. Cocinero,[1] Judith Millán,[2] Anouk M. Rijs,[3,4] Imanol Usabiaga,[1] Alberto Lesarri,[5] Fernando Castaño,[1] and José A. Fernández[1,a)]
[1]*Dpto. de Química Física, Facultad de Ciencia y Tecnología, Universidad del País Vasco-UPV/EHU, B° Sarriena s/n, Leioa 48940, Spain*
[2]*Dpto. de Química, Facultad de Ciencias, Estudios Agroalimentarios e Informática, Universidad de La Rioja, Madre de Dios, 51, Logroño 26006, Spain*
[3]*FOM Institute for Plasma Physics Rijnhuizen, Edisonbaan 14, 3439 MN Nieuwegein, The Netherlands*
[4]*Radboud University Nijmegen, Institute for Molecules and Materials, Toernooiveld 7, 6525 ED Nijmegen, The Netherlands*
[5]*Dpto. de Química Física y Química Inorgánica, Facultad de Ciencias, Universidad de Valladolid, Valladolid 47011, Spain*

(Received 30 May 2012; accepted 26 July 2012; published online 15 August 2012)

Propofol (2,6-di-isopropylphenol) is probably the most widely used general anesthetic. Previous studies focused on its complexes containing 1 and 2 water molecules. In this work, propofol clusters containing three water molecules were formed using supersonic expansions and probed by means of a number of mass-resolved laser spectroscopic techniques. The 2-color REMPI spectrum of propofol · $(H_2O)_3$ contains contributions from at least two conformational isomers, as demonstrated by UV/UV hole burning. Using the infrared IR/UV double resonance technique, the IR spectrum of each isomer was obtained both in ground and first excited electronic states and interpreted in the light of density functional theory (DFT) calculations at M06-2X/6-311++G(d,p) and B3LYP/6-311++G(d,p) levels. The spectral analysis reveals that in both isomers the water molecules are forming cyclic hydrogen bond networks around propofol's OH moiety. Furthermore, some evidences point to the existence of isomerization processes, due to a complicated conformational landscape and the existence of multiple paths with low energy barriers connecting the different conformers. Such processes are discussed with the aid of DFT calculations. © *2012 American Institute of Physics*. [http://dx.doi.org/10.1063/1.4743960]

## INTRODUCTION

Propofol (2,6-di-isopropylphenol, Scheme 1) and its water clusters constitute an interesting case of study for spectroscopists for two reasons. On the one hand, the steric hindrance introduced by the two isopropyl substituents makes the hydroxy moiety less appealing for solvent molecules to establish hydrogen bonds than its homologue phenol and therefore many molecules may prefer the interaction with the $\pi$-cloud of the aromatic ring. Thus, propofol offers the chance to study the competition between two fundamental types of interactions, namely, hydrogen bond (O−H · · · O) and weak hydrogen bond (O−H · · · $\pi$) with contribution from dispersion forces.[1] On the other hand, characterization of the microsolvation of propofol may eventually lead to biologically relevant conclusions, as demonstrated in previous studies.[2,3] Propofol is probably the most widely used non-volatile general anesthetic.[4–6] Once it is injected in the body, most of it is captured by the human serum albumin and travels through the body.[7] A small amount arrives at the brain and finally ~2% of the initially injected propofol crosses the blood-brain barrier. In the central nervous system, propofol is able to attach to gamma amino butyric acid A ($GABA_A$) receptors, acting as agonist and delaying the closing of the ion channel, which results in a blockage of the neuronal impulse.[4,5,8] The docking process is controlled by the difference in Gibbs free energy between propofol solvated by the extracellular medium and propofol interacting with the receptor's active site. Therefore, a deep knowledge of the interactions both inside and outside the cavity will help to understand the docking process.

Previous works have reported on the structure and conformational landscape of bare propofol, propofol · $(H_2O)_{1,2}$, and propofol · phenol complexes using either microwave[9] or IR and UV laser spectroscopy.[2,3] Depending on the conditions of the expansion, it is possible to detect up to four of the five conformers of propofol (Fig. S1 of the supplementary material).[10] The shallow barrier between the two most stable conformers, namely, GG and Gg, can be surmounted if a buffer gas heavier than He is used, so the structure GG is not observed when Ne or Ar are used as carrier gas. Microsolvation with one or two water molecules leads to a reduction on the number of isomers detected by mass-resolved IR and UV spectroscopy: from four in the bare molecule to three in the monohydrated species and to two in the complex with two water molecules. In the latter, both isomers are based in the same propofol conformer and only differ in the orientation of the water molecules.[2] Furthermore, isomerization processes were detected not only in ground but also in the excited electronic state: there is a change in the arrangement of the isopropyl groups upon excitation, leading to the existence of a common excited state for the two propofol most stable isomers.

a)Author to whom correspondence should be addressed. Electronic mail: josea.fernandez@ehu.es. Telephone: + 34 94 601 5387. Fax: + 34 94 601 35 00. URL: https://sites.google.com/site/gesemupv/.

 

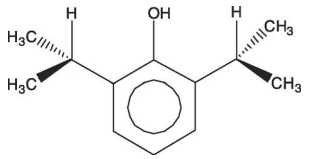


SCHEME 1. Propofol (2,6-di-isopropylphenol).

Such effect is dramatically increased in propofol/phenol clusters, where the isopropyl wagging motions connects several species.[3]

All these systems present a complex spectroscopy, which is also reflected in the difficulty of the calculations to correctly predict the stability of the different species. For example, the lowest calculation level that can correctly predict the relative stability of the bare molecule is MP2/ cc-pVTZ, while both M06-2X/6-311++G(d,p) and MP2/6-311++G(d,p) predict that propofol $\cdot (H_2O)_2$ most stable structures are those with the water molecules forming a hydrogen bond network between propofol's hydroxy group and the $\pi$-cloud of aromatic ring. However, such structures are not detected using high-resolution IR and UV spectroscopy and the two conformers experimentally detected present cyclic cooperative hydrogen bond structure, such as those observed in phenol $\cdot (H_2O)_2$.[11] Furthermore, the success of MP2/cc-pVTZ in predicting the energetic order may well be just due to cancellation errors and further increasing of the base functions may lead to contradictory results.[12]

Following such studies, we present here a spectroscopic study on propofol $\cdot (H_2O)_3$. Addition of a third water molecule raises considerably the number of possible stable structures, although there is still a competition between cyclic and linear cooperative hydrogen-bond networks. In this study, we address the questions of whether water can still form cyclic structures with propofol's hydroxy moiety or if water prefers to self-aggregate and interacts with the aromatic ring. For the latter scenario, water may find a less hostile environment due to its larger cluster-size, as the isopropyl groups cannot shield the ring from interacting with water. Additionally, it will be interesting to discover if an increase of the system's size leads to further reduction on the number of isomers, or if a change in the previous observed tendency takes place. Finally, comparison of the results obtained with those from phenol $\cdot$ water clusters by other groups[11,13–21] allows us to evaluate the influence of the isopropyl groups in the solvation of the chromophore.

## METHODS

### Experimental

Detailed description of the experimental procedure can be found elsewhere.[22,23] Propofol (97%, Sigma-Aldrich) was seeded in He, Ne, and/or Ar without further modifications and the mixture was expanded inside the chamber of a linear time-of-flight (Jordan Inc.). Propofol is liquid at room temperature and therefore it was not necessary to heat the sample to obtain enough vapor pressure. To form the propofol–water clusters, the seed gas flows through a small water reservoir. Water was picked up by the seed gas and clusters were formed in the supersonic expansion. Typical backing pressures of 1–2 bars were employed before the expansion.

The supersonic beam passes through a 2 mm skimmer before entering the ionization chamber of a time-of-flight mass spectrometer (Jordan Inc.) where it is interrogated with a variety of UV and IR laser-based techniques. In the 2-color REMPI experiments, the UV pump laser is tuned to propofol $\cdot (H_2O)_3$ $S_1 \leftarrow S_0$ electronic transition. The excited molecules are further ionized by the UV probe laser, with little excess of energy, avoiding fragmentation and therefore interference from higher order clusters. UV-UV hole-burning spectroscopy was performed using a three-laser scheme. The UV depopulation laser was tuned to the transition to be probed, while the above described 2-color REMPI scheme was used to ionize the formed clusters. The pump/probe laser beams were delayed by 100–400 ns. An active subtraction is also performed to improve *S*/*N* ratio. A similar scheme is employed for the ground state IR/UV ion-dip spectroscopy (IRIDS) experiments, but now using an IR laser for depopulation. The IRIDS experiments require very low power density: usually 100 $\mu$J of a focused IR laser is enough to achieve a 70%–80% depopulation of the REMPI signal. A delay of 100–400 ns was set between the IR and the UV lasers. Excited state IRID experiments were conducted firing the IR laser between the two UV lasers, with delays of 10 ns between UV pump and IR and UV probe lasers.

IR spectra in the mid-IR and fingerprint region (500–1500 $cm^{-1}$) were recorded at the Free Electron Laser for Infrared Experiments (FELIX) at the FOM Institute of Plasma Physics Rijnhuizen.[24] Briefly, the experiments have been carried out in a differentially pumped molecular beam setup equipped with a reflector time-of-flight mass spectrometer.[25] The skimmed free jet enters the ionization region, where it is crossed by counter-propagating IR and UV laser beams. Both the molecular beam and the UV laser beam were running at 10 Hz, while FELIX was running at 5 Hz. In order to minimize signal fluctuations due to long-time drifts in the UV laser power or source conditions, a normalized ion-dip spectrum is obtained by recording separately the alternating IR-off and IR-on signals. Additionally, the IR spectra are corrected for the intensity variations on the IR power over the complete wavelength range.

### Calculations

Density functional theory (DFT) calculations were conducted using GAUSSIAN 09 suite[26] running on the supercomputers in the UPV/EHU computation facility and in the i2BASQUE Foundation. A conformational search was done using molecular mechanics (MMFFs) and a number of algorithms for structure generation (large amplitude-low mode and Monte Carlo), as implemented in Macromodel (Schrodinger Inc.). A minimum of 100 000 runs were performed, obtaining thousands of candidate structures, most of them redundant. Such structures were grouped into families attending to their similarity. Those structures in a 25 kJ/mol stability window, together with representative structures from each family were selected for further optimization at the

M06-2X/6-311++G(d,p) level. Twenty-four fully optimized structures were obtained in this way (Fig. S2 of the supplementary material). All the structures were tested to be true minima running a normal mode analysis and looking for the absence of negative frequencies. All the energy values given in this work are zero point energy corrected. Table S1 of the supplementary material[10] collects the binding energy values for the calculated propofol $\cdot (H_2O)_3$ clusters. Such values are corrected for the basis-set superposition error (BSSE) using the Boys and Bernandi counterpoise method.[27] The final structures are named as s1, s2, s3,. . . , etc., where the number refers to their energetic order, being s1 the global minimum.

During this work, the meta-DFT method M06-2X was chosen for most of the calculations, as it is able to describe the interactions due to dispersive forces,[28] which may be important in some of the calculated structures. However, such functional is computationally more expensive, compared with other functionals, such as B3LYP, which works reasonably well when only hydrogen bond interactions are into play. Thus the latter was employed together with the 6-311++G(d,p) basis set for the exploration of several reaction coordinates, in which the main interaction is due to hydrogen bond. The exploration of reaction coordinates requires of a considerably large number of iterations and a large number of points were calculated for each coordinate. Thus, employing B3LYP instead of M06-2X results in a considerable reduction on the calculation time.

## RESULTS AND DISCUSSION

### Conformational landscape exploration

Propofol has a complicated conformational landscape for a molecule of its size, due to the flexibility of its isopropyl groups that raise five conformational possibilities, namely, Gg (global minimum), GG, EG, GE, and EE (Fig. S1 of the supplementary material).[10] The water molecules are expected to stabilize more of those bare molecule conformers in which the hydroxy group is more exposed (i.e., conformers GG and Gg, which are in turn the two most stable conformers). Figure 1 shows a ball and stick representation of the eight most stable calculated species of propofol $\cdot (H_2O)_3$, while the rest of the optimized structures can be found in Fig. S2 of the supplementary material,[10] together with their relative stability, binding energy, zero-point energy (ZPE), and BSSE (Table S1).[10] All the structures in Fig. 1 are stabilized by cooperative hydrogen bond networks between the water molecules and hydroxy group and/or $\pi$-cloud of propofol. The global minimum (s1) and structure s5 present a hydrogen bond network between propofol's hydroxy group and the aromatic ring. Almost isoenergetical with the global minimum are structures in which the water molecules form an eight-member ring built around the hydroxy group, which can be either in the same plane than the aromatic ring (s3) or perpendicular to it (s2, s4, and s6). Meanwhile, structures s7 and s8 form a six-member ring with two water molecules and propofol's hydroxy group, while the third water is interacting with the $\pi$-cloud of propofol. The calculations predict a loss of stability around 5–6 kJ/mol for such structures compared with the global minimum. Nevertheless, taking into account the system's size, the energy difference between the structures in Fig. 1 is small enough to expect most of them to be present in the expansion, provided that there are no low energy barriers that allow a conformational relaxation in the jet.

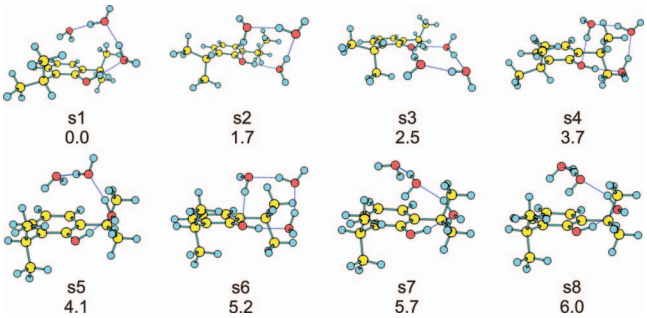


FIG. 1. Eight most stable structures of propofol $\cdot (H_2O)_3$ as calculated at the M06-2X/6-311++G(d,p) level. Relative energies in kJ/mol.

It is worthy to note that propofol adopts a conformation mid way between GG and Gg in the calculated global minimum (structure s1), as one of the isopropyl hydrogen atoms is in the plane of the ring, and that the other three most stable structures are based on a GG-propofol core. The next four structures, following the energetic sequence, are built on EG-propofol cores and only above 6.0 kJ/mol (structure s9) it is possible to find structures with the bare molecule adopting a Gg conformation. The structures based on conformer EE (the one with the most shielded OH group) are predicted to be >12 kJ/mol above the global minimum (s17).

### Spectroscopy

Figure 2 shows the 2-color REMPI spectra of propofol $\cdot (H_2O)_{0\text{-}3}$ in the 36 000–37 000 $cm^{-1}$ region. At first glance, there is a reduction in the vibrational activity with the addition of the third water molecule, and the spectrum extends for no more than 250 $cm^{-1}$. Also, the trend in the variation of the position of the $0_0^0$ transition with the number of water molecules points to formation of a cyclic water structure, as it happens for the doubly hydrated species. Replacing the He carrier gas by Ne leads to disappearance of some features in the 36 100–36 200 $cm^{-1}$ region of the spectrum. A similar behavior was observed for bare propofol and propofol $\cdot (H_2O)_1$, due to population migration from one of the isomers to a more stable species. Therefore, the spectra in Fig. 2 point to the existence of at least two isomers, separated by shallow energy barriers and with the water molecules forming a cyclic hydrogen bond network around propofol's hydroxy moiety. Such observations are in agreement with the results from the UV/UV hole burning (Fig. 3), which clearly show the existence of two conformers with $0_0^0$ transitions at 36 185 and 36 255 $cm^{-1}$. The hole-burning experiment also shows that both conformers present very different vibrational activity: while the spectrum of conformer 1 shows a very small number of discrete features, extending for no more than ~40 $cm^{-1}$, the spectrum of conformer 2 exhibits strong transitions forming progressions during ~70 $cm^{-1}$.

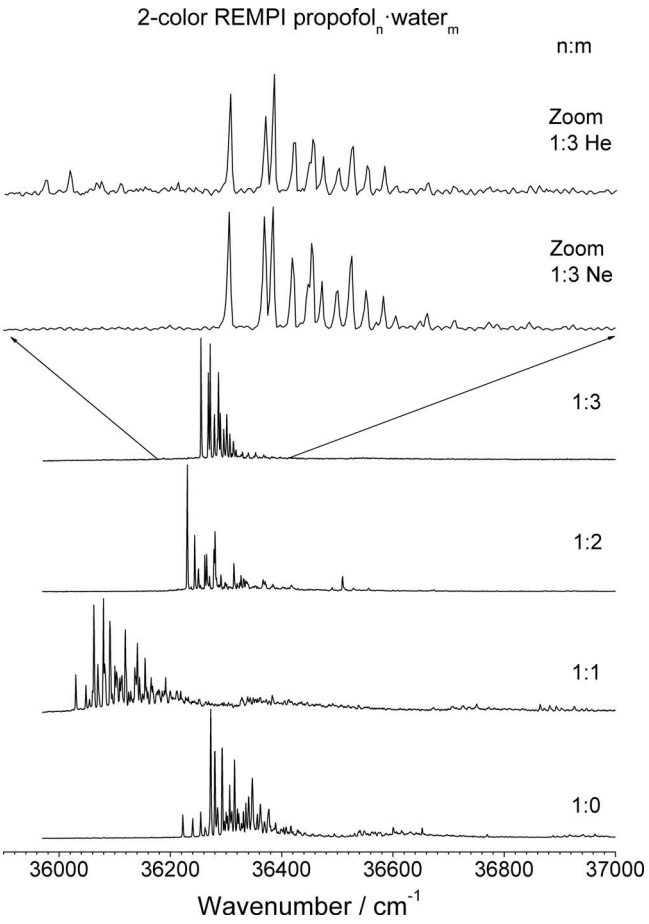


FIG. 2. Two-color REMPI spectra of propofol · $(H_2O)_n$, n = 0–3 obtained in a supersonic expansion of propofol/water in 2 bars of He and with the probe laser tuned at 27 972 cm$^{-1}$. The zoom also offers a comparison between the spectra of propofol · $(H_2O)_3$ obtained using He and Ne. Disappearance of some features is observed, probably due to population transfer between isomers.

The IR spectrum of the two detected isomers was recorded both in the mid-IR/fingerprint and OH stretching regions, following the procedure described in the Experimental section (Fig. 4). The spectra of the two isomers in the 3100–3800 cm$^{-1}$ region are very similar, which suggests that they have similar structures. Three broad, strong peaks are observed in the 3200–3500 cm$^{-1}$ region, accompanied by a weaker band at 3408 cm$^{-1}$ for isomer 1 and at 3348 cm$^{-1}$ for isomer 2. These 3–4 bands correspond to $\sigma$(OH) vibrations of hydrogen bonded water and propofol and are separated from the free $\sigma$(OH) bands at ∼3710 cm$^{-1}$ by an empty spectral region, usually called the *window region*,[29,30] which is associated with the formation of ring-like hydrogen bond networks.

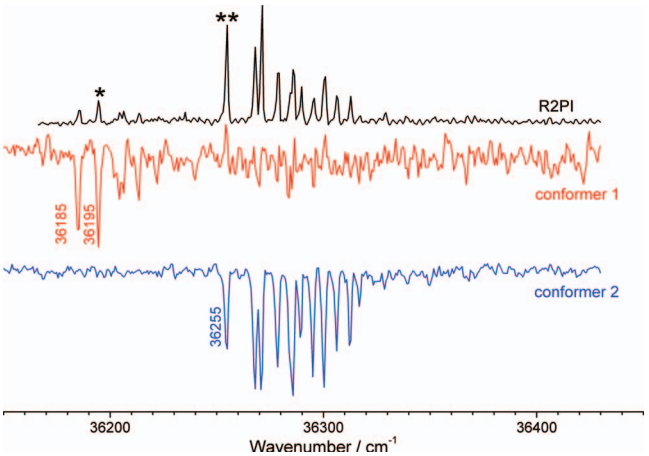


FIG. 3. Comparison between propofol · $(H_2O)_3$ 2-color REMPI spectrum and the hole-burning traces obtained tuning the probe laser at 36 195 (*) and 36 255 cm$^{-1}$ (**), respectively. Two isomers are detected in the expansion.

## Structural assignment

Figure 4 shows the predicted spectra for some representative calculated structures, while the whole set of predicted spectra are collected in Fig. S3 of the supplementary material.[10] It is clear from the comparison with the experimental data, that the structures in which a water molecule is interacting with the aromatic ring (for example, s1, the most stable calculated structure, s7, s9, s15, and s19) are not able to reproduce the experimental results, as they present a number of transitions in the so-called window region between 3500–3700 cm$^{-1}$, while no band is observed in the experimental traces. One must take into account in doing the assignment that the predicted intensity for the bands in such region is usually weaker than in the actual experimental spectrum.

Among the calculated structures with cyclic water arrangements s6, which is based in propofol's EG conformer, is not able to correctly predict the experimental spectra. Thus, only s2 and s3 are able to correctly reproduce the window region observed in the experimental spectra, and therefore the experimental spectra are assigned to these two structures (see also Fig. S3). In addition, s2 and s3 are among the most stable calculated structures.

Certainly, the predicted spectra show four strong, well-resolved features in the 3300–3450 cm$^{-1}$ region, while only three are clearly resolved in the experimental traces, although they are broad enough to hide the fourth peak, which may be assigned to one of the shoulders of the main peaks.

Both s2 and s3 assigned structures are based on propofol's GG conformer with the water molecules forming an eight-member ring. The difference between both structures is the orientation of the ring of waters respect to the aromatic ring: in plane for s3 or perpendicular to the aromatic ring for structure 2. Unfortunately, both structure s2 and s3 result in similar spectra in the 3 $\mu$m IR region, hampering a more precise assignment.

Regarding the IR spectra obtained in the 500–1700 cm$^{-1}$ region with the free electron laser, a larger spectral congestion is observed due to the appearance of several ring deformation and isopropyl bending vibrations, together with collective vibrations from the hydrogen bond network. Once more, structures s2 and s3 correctly predict the general features of the experimental traces. Unfortunately, also in this IR region their spectra are too similar to perform a more precise assignment.

It is possible to record the IR spectra of the first excited electronic state ($S_1$) by changing the IR and UV lasers firing sequence, as explained in the Methods section. Figure 5 shows a comparison between the $S_0$ and $S_1$ IR spectra of both detected conformers. Propofol, as phenol, is a photo-acid,

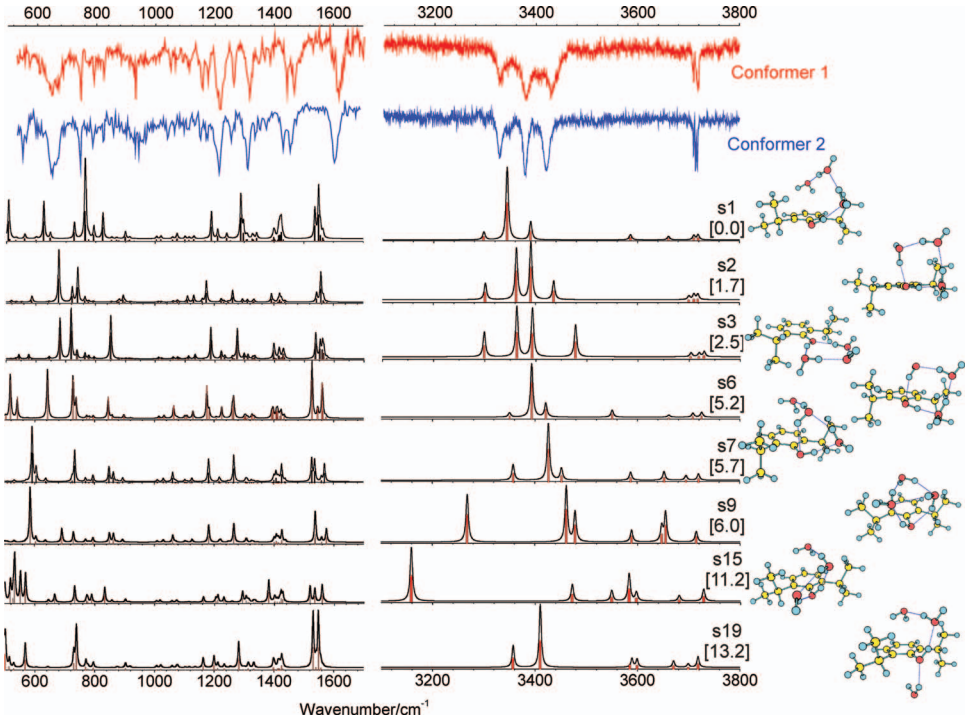


FIG. 4. Comparison between the experimental IR/UV traces obtained for the two detected propofol $\cdot (H_2O)_3$ conformers and the predicted spectra for some representative structures. Comparison with the complete set of calculated structures can be found in Fig. S3 of the supplementary material.[10] A correction factor of 0.938 was employed to account for the anharmonicity.

and therefore electronic excitation usually leads to a red shift in the stretching vibration of its OH moiety.[16] Furthermore, in systems with cyclic hydrogen bond networks, such as phenol $\cdot (H_2O)_3$, a red shift of at least two of the $\sigma$(OH) vibrations is usually observed, as all the hydrogen bonds are reinforced upon excitation.[16] Conversely, only blue shifts are observed for propofol $\cdot (H_2O)_3$ upon excitation. Nevertheless, due to a strong coupling between the vibrations of all the OH moieties, it is not possible to isolate the $\sigma$(OH) of propofol in the spectra in Fig. 5. Figure S4 of the supplementary material[10] shows sketches of all seven collective $\sigma$(OH) vibrations for structures s2 and s3. On the other hand, the bands in the 3300–3600 $cm^{-1}$ on the $S_1$ spectrum (specially for isomer 2) are narrower than in $S_0$, pointing to a better coupling between the OH stretch vibrations in the excited state.

Another striking characteristic of the $S_1$ IR spectrum of conformer 1 is the appearance of several additional peaks around ~3512 $cm^{-1}$. Apparently, one of the bands is composed of 4–5 peaks, separated 8, 11, and 8 $cm^{-1}$, respectively. The origin of these features is unclear, but it could result from an isomerization process in the excited state or the existence in the expansion of several species with overlapping $S_1 \leftarrow S_0$ transitions, but with slightly different $S_1$ IR spectra. Both effects were observed earlier for propofol and its mono and doubly hydrated clusters,[2] and therefore likely to be present in propofol $\cdot (H_2O)_3$ as well.

Finally, the stretches of the free OH are not affected by the electronic excitation, as observed for similar systems.[15]

To explain the spectra in Fig. 5, we have carried out a calculation on the excited state of the two assigned structures, s2, s3, and on s1, the global minimum. Using the ground state geometries, a full optimization was carried out on each structure at CIS/6-31G(d,p) level, followed by a normal mode analysis at the same theory level. Optimization of excited state structures is considerably more complex than in the electronic ground state. Thus, the calculation level employed is relatively modest, but increasing on the basis set size always resulted in a lack of convergence of the calculations. To compare experimental and predicted spectra, a correction factor of 0.88 was applied to the calculated frequencies, and was chosen to adjusts the position of the free OH stretches. As can be seen, such correction factor is considerably lower than the one employed for the ground electronic state, confirming once more that the calculation level employed yields a less accurate description of the system.

The calculated frequencies in Fig. 5 qualitatively reproduce the two groups observed in the experimental traces and the blue shift of the frequencies in the excited state, but the difference with the experimental spectra is larger than the differences between predicted spectra, and therefore they do not help in the assignment.

## Potential energy surfaces

In order to further investigate the origin of the splitting in the $S_1$ IR spectrum, and to explain the depopulation observed with Ne in Fig. 2, a number of calculations were carried out. Figure 6 shows the potential energy curve (PEC) of the ground state obtained taking the GG-based conformer s2 and rotating the isopropyl group on the right in 30° steps, while the rest of the coordinates are relaxed (rotating the other isopropyl group results in a similar PEC, as the ring of

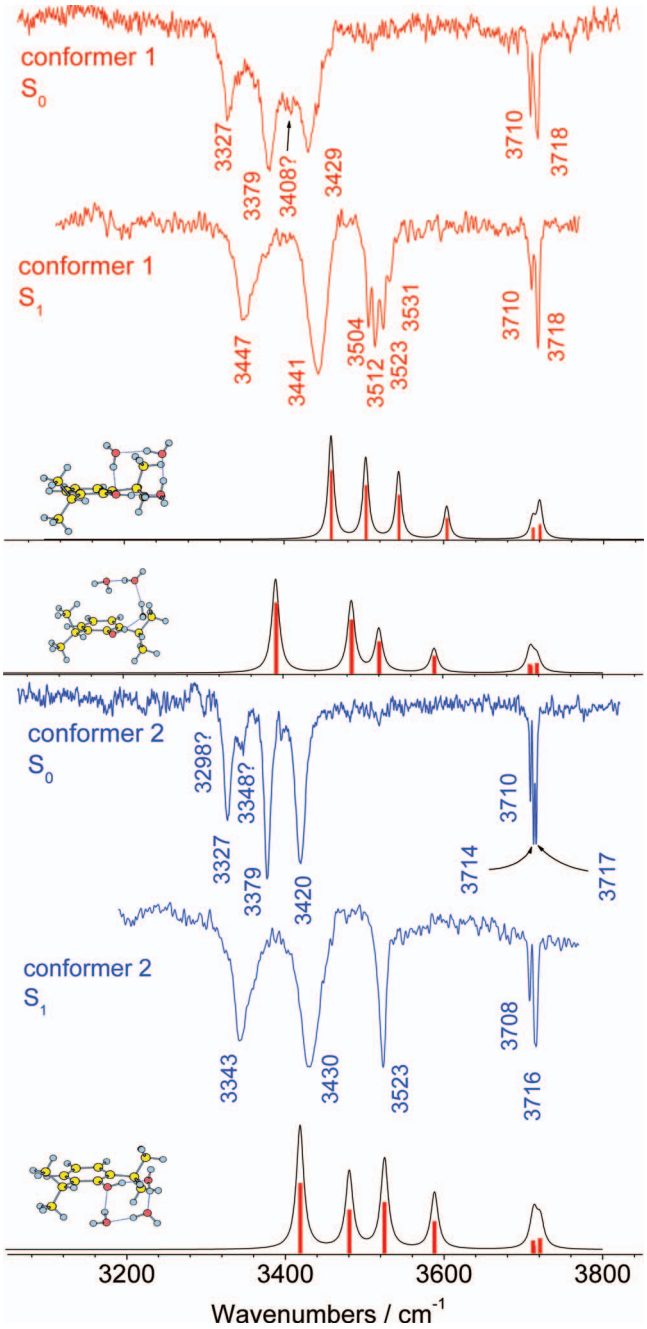


FIG. 5. Comparison between the experimental IR/UV traces obtained for the two detected propofol $\cdot (H_2O)_3$ in ground and excited electronic states. The calculated spectra for the structures s1, s2, and s3 in their first excited electronic state are also included. CIS/6-31G(d,p) calculation level was employed in the excited state calculation. Also, a correction factor of 0.88 was used to account for the anharmonicity.

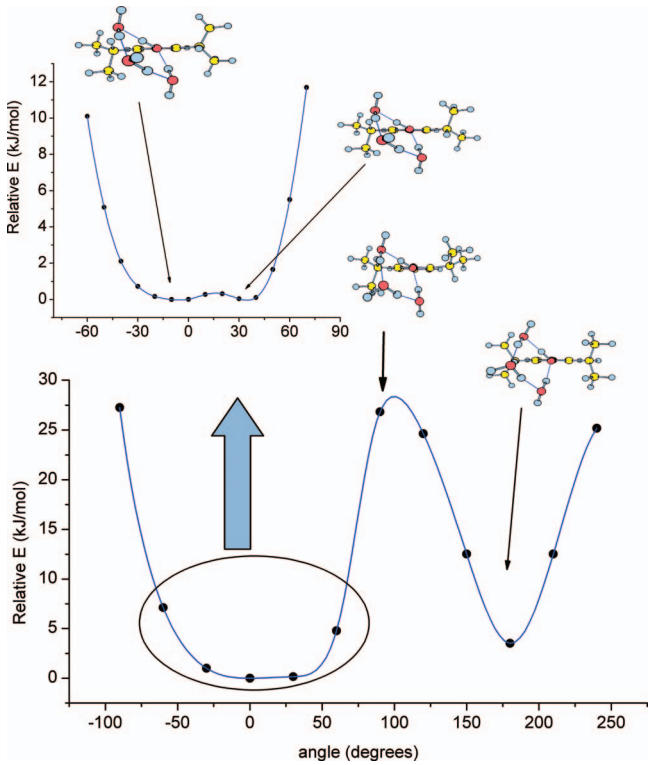


FIG. 6. (Lower panel) Electronic ground state potential energy curve obtained using the calculated structure s2 as starting point and rotating the isopropyl group on the right in 30º steps, while the rest of the coordinates are relaxed. (Upper panel) A more detailed scan around the global minimum was performed, rotating the same isopropyl group in 10° steps. Two shallow minima separated by a very small barrier are found. Calculations performed at B3LYP/6-311++G(d,p) level. The blue lines represent a spline fit, added as an eye guide.

waters moves synchronously with the isopropyl groups). A broad minimum is obtained, which contains several species. A more precise scan was performed around the minimum, taking 10º steps. In this case, two minima are clearly seen, separated by a ∼0.2 kJ/mol barrier and therefore such barrier is lower than the ZPE of the vibrations involve in this coordinate. Interestingly, the structure based on Gg-propofol is not found in this search. The same kind of topography is observed when s3 is taken as starting point (Fig. S5 of the supplementary material),[10] although in this case, the Gg-propofol based isomer is the global minimum and the GG-propofol based s2 structure is not reached. The PECs presented in Figs. 6 and S5 demonstrate that very small differences in the starting optimization geometry result in a different optimized GG/Gg-propofol based structure, demonstrating once more that the barriers separating such minima are small. A more exhaustive calculation involving multiple degrees of freedom would be required to map the paths connecting all the minima. Such calculation is beyond the scope of the present study. Nevertheless, we can conclude that the depopulation observed with Ne is not due to population transfer between GG/Gg-based propofol $\cdot (H_2O)_3$ conformers, as the barriers between such structures are too small to be able to isolate both species in the beam. On the other hand, the structural differences between structures s2 and s3 require more complicate rearrangements during the isomerization process, and therefore the barriers separating them are high enough to find the two minima, as demonstrated experimentally. Furthermore, as there is population migration during the cooling process with Ne, such barriers may not be higher than ∼5 kJ/mol.[31] However, finding the path connecting those two minima is not straightforward. We scanned the rotation of propofol's hydroxy group in the $S_0$ state using either s2 or s3 as starting structures (Figs. S6 and S7 of the supplementary material)[10] and although a barrierless path could not be found, certainly both minima are connected through such coordinates. Therefore, it is very likely

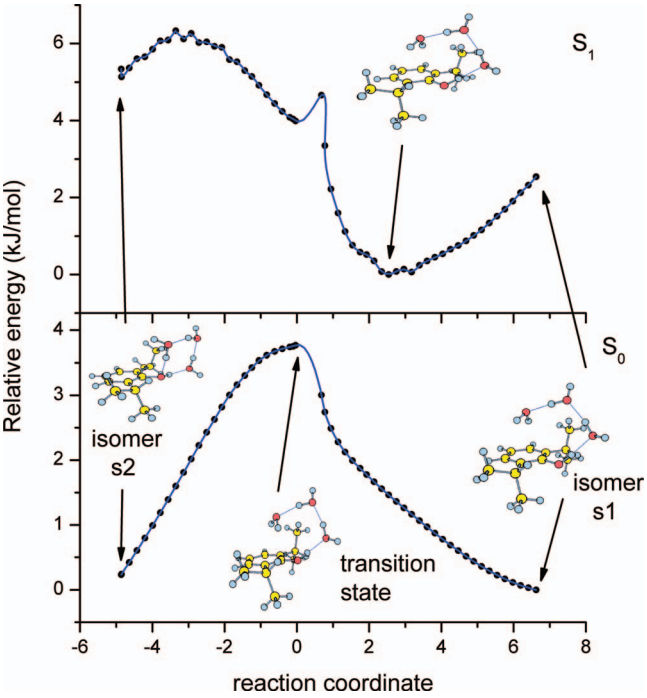


FIG. 7. (Lower panel) Reaction coordinate scan from structure s2 to s1 in the electronic ground state, calculated at M06-2X/6-311++G(d,p) level. A true transition state was located. (Upper panel) Estimation of the same reaction path in the first excited electronic state, built running a single point TD-DFT calculation on each structure of the $S_0$ path. The blue lines represent a spline fit, added as an eye guide.

that adding further degrees of freedom to our search, a reaction path whose barriers may be surmounted by collisions with Ne may be found.

### Electronic origins' observed shifts

The observed trends in the shifts on the electronic origins of the detected conformers also deserve some attention. As explained above, formation of ring-like structures usually result in a blue shift with the increase in the number of components. Certainly, conformer 2 follows such trend. However, conformer 1 presents a red shift respect to the 1:2 species. On the other hand, it has been already demonstrated that electronic excitation induces conformational changes in this system[2] and that may well be the present case, hampering a precise location of the $0_0^0$ transition. In such situation, the more likely explanation for the observed shifts is the opening of the water ring, also postulated for other systems.[15] Figure 7 (lower panel) shows the $S_0$ reaction path that connects (ring-like) s2 with (open ring) s1, calculated at the M06-2x/6-31++G(d,p) level. As can be seen, a small barrier of ~3.5 kJ/mol was found in the electronic ground state. A TD-DFT calculation was carried out in each of the points of the ground electronic state reaction path, in order to have a rough estimation of such path in the excited state (Fig. 7, upper panel). The energy order of structures s2 and s1 changes upon excitations, becoming an s1-like structure considerably more stable. In addition, the barrier to move from s2 to the s1-like structure decreases to slightly more than 1 kJ/mol. Such small barrier is in good agreement with the shape of conformer 1 electronic spectrum (Fig. 3), whose discrete features extend for ~40 $cm^{-1}$. Thus, electronic excitation may lead to an isomerization, which may be also the origin of the multiplet observed in Fig. 5. Hence, this evidence leads us to assign isomer 1 to the calculated structure s2 and isomer 2 to s3.

TABLE I. Band origins and frequencies ($cm^{-1}$) of the observed OH stretching vibrations of propofol · $(H_2O)_3$ and phenol · $(H_2O)_3$.

| | Propofol · $(H_2O)_3$ | | |
|---|---|---|---|
| | Isomer 1 | Isomer 2 | Phenol · $(H_2O)_3$ |
| $0_0^0$ | 36 185 | 36 255 | 36 261[a] |
| **$S_0$** | | | |
| | 3327 | 3327 | 3236[b] |
| | 3379 | 3348?[c] | 3345[b] |
| | 3408?[d] | 3379 | 3401[b] |
| | 3429 | 3420 | 3451[b] |
| | 3710 | 3710 | 3715[b] |
| | 3718[e] | 3714 | 3719[b] |
| | | 3717 | 3722[b] |
| **$S_1$** | | | |
| | 3347 | 3343 | 3325[b] |
| | 3441 | 3430 | 3435[b] |
| | 3504, 3512, 3523, 3531[f] | 3523 | 3515[b] |
| | 3710 | 3708 | 3713[b] |
| | 3718 | 3716 | 3719[b] |
| | | | 3725[b] |

[a]Reference 32.
[b]Reference 16.
[c]Shoulder.
[d]Small peak.
[e]This is probably a combination of two bands.
[f]Multiplet.

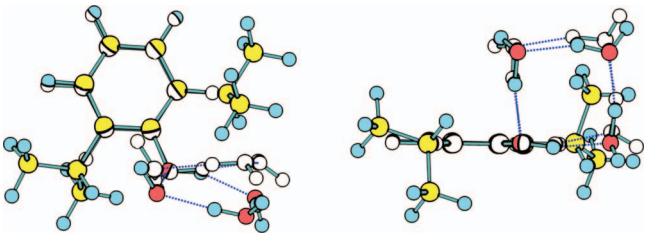

FIG. 8. Comparison between the calculated structures of propofol $\cdot (H_2O)_3$ s2 and phenol $\cdot (H_2O)_3$ at M06-2X/6-311++G(d,p). The atoms of phenol $\cdot (H_2O)_3$ are shown as white spheres.

Regarding the observed shift for isomer 2 (structure s3), it does follow the expected trend, probably due to the similarity of its structure with that of propofol $\cdot (H_2O)_2$, in which the water molecules form an in-plane 6-member ring with propofol's hydroxy moiety.[2]

### Comparison with phenol clusters

The comparison of propofol $\cdot (H_2O)_3$ observed species with those detected for phenol allows an evaluation of the isopropyl groups on the solvation process. Table I collects the position of the $0_0^0$ transitions for the two isomers detected and the position of the $\sigma$(OH) vibronic bands in the IR spectra for propofol $\cdot (H_2O)_3$, together with the data reported in the literature for phenol $\cdot (H_2O)_3$. According to Table I, the OH stretches in propofol $\cdot (H_2O)_3$ lie closer together than in phenol, which points to smaller differences between the hydrogen bonds. A comparison between propofol $\cdot (H_2O)_3$ isomer 2 and phenol $\cdot (H_2O)_3$ structures (Fig. 8) shows that the ring of waters is repelled by one of the isopropyl groups, and therefore it cannot reach the optimal geometry, decreasing the system's stability. Such structural difference may in addition facilitate ring opening upon electronic excitation.

Nevertheless, the most striking difference between phenol $\cdot (H_2O)_3$ and propofol $\cdot (H_2O)_3$ clusters is the coexistence in the expansion of two isomers of the later, while only one isomer is found for the former. Thus, introduction of the isopropyl groups increases the number of species, increasing the entropy of the system.

### Conclusions

In this work, we analyze the spectroscopy of propofol $\cdot (H_2O)_3$ using a number of mass-resolved spectroscopic techniques. Two isomers are found to compose the 2-color REMPI spectrum, using hole-burning spectroscopy, with $0_0^0$ transitions at 36 185 and 36 255 $cm^{-1}$. Comparison between the experimental IR/UV spectra obtained both in the $\sigma$(OH) and mid-IR/fingerprint regions and the spectra predicted for the structures calculated at M06-2X/6-311++G(d,p) level lead to assign conformer 1 to s2, a structure with the water molecules forming a ring in a plane perpendicular to the aromatic ring, and conformer 2 to s3, in which the ring of waters are in the same plane than the aromatic ring. Therefore, although the isopropyl groups cannot shield the OH moiety from interacting with water, they give raise to two isomers, while in phenol $\cdot (H_2O)_3$ only the equivalent structure to s2 is detected.

A number of calculations are carried out to explain the population migration between conformers 1 and 2 and the changes observed in the IR spectra upon electronic excitation. The calculations point to the existence of paths with small energy barriers connecting s2 and s3. Also, calculations show that the electronic excitation favors transition from s2 to s1 structures, i.e., water-ring opening. Such mechanism may explain the blue shift observed in the IR spectrum of conformer 1 and the appearance of a multiplet around 3512 $cm^{-1}$ in the $S_1$ IR spectrum.

Analysis of higher propofol/water clusters is already in progress.

### ACKNOWLEDGMENTS

The research leading to these results has received funding from the European Community's Seventh Framework Programme (FP7/2007-2013) under Grant No. 226716 and Spanish Ministry of Science and Innovation-MICINN (Consolider-Ingenio 2010/CSD2007-00013 and CTQ2009-14364/ CTQ2011-22923). We would like to thank the staff of FELIX for their support during the experiment. Technical and human support provided by the Laser Facility of the SGIKER (UPV/EHU, MICINN, GV/EJ, ESF) is also gratefully acknowledged. I.L. thanks the GV for a predoctoral fellowship; E.J.C. also acknowledges a "Ramón y Cajal" contract from the MICINN. Computational resources from the SGI/IZO-SGIker and i2BASQUE were used for this work. J.M. thanks the UR for the additional support (API09/10).

[1] G. R. Desiraju and T. Steiner, *The Weak Hydrogen Bond in Structural Chemistry and Biology* (Oxford University Press, Oxford, 2001).
[2] I. Leon, E. Cocinero, J. Millan, S. Jaeqx, A. M. Rijs, A. Lesarri, F. Castano, and J. A. Fernandez, Phys. Chem. Chem. Phys. **14**, 4398 (2012).
[3] I. Leon, J. Millan, E. Cocinero, A. Lesarri, F. Castano, and J. A. Fernandez, Phys. Chem. Chem. Phys. **14**, 8956 (2012).
[4] P. Arhem, G. Klement, and J. Nilsson, Neuropsychopharmacology **28**, S40–S47 (2003).
[5] *Molecular and Basic Mechanisms of Anesthesia*, edited by B. W. Urban and M. Barann (Pabst Science, Lengerich, 2002).
[6] L. L. Brunton, J. S. Lazo, and K. L. Parker, *The Pharmalogical Basis of Therapeutics* (McGraw-Hill, New York, 2006).
[7] A. A. Bhattacharya, S. Curry, and N. P. Franks, J. Biol. Chem. **275**, 38731 (2000).
[8] N. P. Franks and W. R. Lieb, Nature (London) **367**, 607 (1994).
[9] A. Lesarri, S. T. Shipman, J. L. Neill, G. G. Brown, R. D. Suenram, L. Kang, W. Caminati, and B. H. Pate, J. Am. Chem. Soc. **132**, 13417 (2010).
[10] See supplementary material at http://dx.doi.org/10.1063/1.4743960 for all the calculated structures, predicted vibrational spectra, tables with the binding energies, and potential energy curves.
[11] A. Luchow, D. Spangenberg, C. Janzen, A. Jansen, M. Gerhards, and K. Kleinermanns, Phys. Chem. Chem. Phys. **3**, 2771 (2001).
[12] M. Kolar and P. Hobza, J. Phys. Chem. A **111**, 5851 (2007).
[13] G. Berden, W. L. Meerts, M. Schmitt, and K. Kleinermanns, J. Chem. Phys. **104**, 972 (1996).
[14] T. Ebata, M. Kayano, S. Sato, and N. Mikami, J. Phys. Chem. A **105**, 8623 (2001).
[15] T. Ebata, A. Fujii, and N. Mikami, Int. J. Mass. Spectrom. Ion Process. **159**, 111 (1996).
[16] T. Ebata, N. Mizuochi, T. Watanabe, and N. Mikami, J. Phys. Chem. **100**, 546 (1996).
[17] M. Gerhards, A. Jansen, C. Unterberg, and K. Kleinermanns, Chem. Phys. Lett. **344**, 113 (2001).
[18] M. Gerhards and K. Kleinermanns, J. Chem. Phys. **103**, 7392 (1995).

[19]C. Jacoby, W. Roth, M. Schmitt, C. Janzen, D. Spangenberg, and K. Kleinermanns, J. Phys. Chem. A **102**, 4471 (1998).
[20]R. Parthasarathi, V. Subramanian, and N. Sathyamurthy, J. Phys. Chem. A **109**, 843 (2005).
[21]W. Roth, M. Schmitt, C. Jacoby, D. Spangenberg, C. Janzen, and K. Kleinermanns, Chem. Phys. **239**, 1 (1998).
[22]A. Longarte, C. Redondo, J. A. Fernandez, and F. Castano, J. Chem. Phys. **122**, 164304 (2005).
[23]A. Longarte, I. Unamuno, J. A. Fernandez, F. Castano, and C. Redondo, J. Chem. Phys. **121**, 209 (2004).
[24]D. Oepts, A. F. G. van der Meer, and P. W. van Amersfoort, Infrared Phys. Technol. **36**, 297 (1995).
[25]A. M. Rijs, E. R. Kay, D. A. Leigh, and W. J. Buma, J. Phys. Chem. A **115**, 9669 (2011).
[26]M. J. Frisch, G. W. Trucks, H. B. Schlegel, G. E. Scuseria, M. A. Robb, J. R. Cheeseman, G. Scalmani, V. Barone, B. Mennucci, G. A. Petersson, H. Nakatsuji, M. Caricato, X. Li, H. P. Hratchian, A. F. Izmaylov, J. Bloino, G. Zheng, J. L. Sonnenberg, M. Hada, M. Ehara, K. Toyota, R. Fukuda, J. Hasegawa, M. Ishida, T. Nakajima, Y. Honda, O. Kitao, H. Nakai, T. Vreven, J. A. Montgomery, Jr., J. E. Peralta, F. Ogliaro, M. Bearpark, J. J. Heyd, E. Brothers, K. N. Kudin, V. N. Staroverov, R. Kobayashi, J. Normand, K. Raghavachari, A. Rendell, J. C. Burant, S. S. Iyengar, J. Tomasi, M. Cossi, N. Rega, J. M. Millam, M. Klene, J. E. Knox, J. B. Cross, V. Bakken, C. Adamo, J. Jaramillo, R. Gomperts, R. E. Stratmann, O. Yazyev, A. J. Austin, R. Cammi, C. Pomelli, J. W. Ochterski, R. L. Martin, K. Morokuma, V. G. Zakrzewski, G. A. Voth, P. Salvador, J. J. Dannenberg, S. Dapprich, A. D. Daniels, O. Farkas, J. B. Foresman, J. V. Ortiz, J. Cioslowski, and D. J. Fox, GAUSSIAN 09, Revision A02, Gaussian, Inc., Wallingford, CT, 2009.
[27]S. F. Boys and F. Bernardi, Mol. Phys. **19**, 553 (1970).
[28]Y. Zhao and D. Truhlar, Theor. Chem. Acc. **119**, 525 (2008).
[29]N. Mikami, Bull. Chem. Soc. Jpn. **68**, 683 (1995).
[30]H. Watanabe and S. Iwata, J. Chem. Phys. **105**, 420 (1996).
[31]R. S. Ruoff, T. D. Klots, T. Emilsson, and H. S. Gutowsky, J. Chem. Phys. **93**, 3142 (1990).
[32]A. Oikawa, H. Abe, N. Mikami, and M. Ito, J. Phys. Chem. **87**, 5083 (1983).